A Study of the Growth of the Wave Spectrum with Fetch

KIMMO K. KAHMA

Institute of Marine Research, 00141 Helsinki, Finland

(Manuscript received 3 March 1981, in final form 19 August 1981)

ABSTRACT

The development of the wave spectrum with fetch in a steady wind has been studied with a line of consecutive wave buoys in the Bothnian Sea in 1976 and 1979. The relationship that was found between dimensionless peak frequency $\tilde{\omega}_m$ $(=\omega_m U_{10}/g)$ and dimensionless fetch $\tilde{X}$ $(=gX/U_{10}^2)$ was close to previous observations. The dimensionless energy $\tilde{\sigma}^2$ $(=g^2\sigma^2/U_{10}^4)$ was about twice that observed in the JONSWAP experiment.

In the saturation range when $\tilde{\omega} < 4$ the frequency spectrum was found to have the form $S(\omega) = \alpha_u U_{10} g \omega^{-4}$, where $\alpha_u = 4.5 \times 10^{-3}$, independent of the dimensionless fetch $\tilde{X}$. The deviation from the Phillips −5 power law could not be explained by the influence of currents or finite depth. Near the peak, the spectra were satisfactorily described by the JONSWAP spectrum; above frequencies twice the peak frequency the difference becomes significant. A qualitative explanation is proposed for the dependence of the spectrum on the wind speed in the saturation range. The semi-theoretical method of Longuet-Higgins (1969) to estimate the Phillips saturation-range constant is applied to estimate α_u. The result $(4.4\text{–}6.4) \times 10^{-3}$ agrees with the experimental value. The growth of a component of the dimensionless spectrum with the fetch was found to be exponential within the accuracy of the data. The exponential growth parameter agreed with previous observations. A simple model is proposed to predict the growth rate without assuming nonlinear transfer of energy by wave-wave interactions; the results agree well with observations.

1. Introduction

The development of the wave spectrum in fetch-limited conditions has been studied using a line of consecutive wave buoys. As the experiment lasted seven months, it was possible to make measurements during an exceptionally long period of steady offshore wind, which occurred between 11 and 19 October 1976.

An effective tool in studying the properties of the wave spectrum is the Kitaigorodskii similarity law (e.g., Kitaigorodskii, 1970). In the case of a homogeneous and stationary wind blowing from an approximately straight shoreline the wave spectrum $S(\omega)$ has the form

$$S(\omega) = g^2\omega^{-5}\tilde{S}(\tilde{\omega}, \tilde{X}), \quad (1)$$

where

- g acceleration of gravity
- ω (angular) frequency $[=2\pi f]$
- U_∞ mean wind speed at the upper boundary of the surface boundary layer
- $\tilde{\omega}$ dimensionless (angular) frequency $[=\omega U_\infty/g]$
- $\tilde{X}$ dimensionless fetch $[=gX/U_\infty^2]$
- $\tilde{S}$ dimensionless wave spectrum.

In particular, the dimensionless square root of the variance of surface displacement $\tilde{\sigma} = g\sigma/U_\infty^2$ where $\sigma^2 = \int_0^\infty S(\omega)d\omega$, and the dimensionless peak frequency $\tilde{\omega}_m = \omega_m U_\infty/g$ under these assumptions, are functions of $\tilde{X}$ only.

U_∞, the wind speed at an altitude no longer affected by the energy and momentum transfer from the atmosphere to the waves, must in practice be replaced by some measured quantity. The friction velocity u_* has previously been widely used as a scaling wind speed. However, as pointed out by Hasselmann *et al.* (1973) and Benilov *et al.* (1978b), the large energy and momentum transfer from the atmosphere to the developing waves probably alters u_* and the wind profile, and therefore no local value of u_* is suitable as an independent variable. This is perhaps also true of the wind speed U_{10} at 10 m altitude, but according to Benilov *et al.* (1978b) the variability of U_{10}/U_∞ is considerably less than the variability of u_*/U_∞. We therefore replace U_∞ by U_{10}, as was done in the JONSWAP experiment (Hasselmann *et al.*, 1973, hereafter referred to as JONSWAP).

2. The experiment

The main experiment was carried out in the southern part of the Bothnian Sea in 1976 (Fig. 1). A profile from four consecutive wave buoys was used to measure the wave growth in offshore wind

0022-3670/81/111503-13$07.25

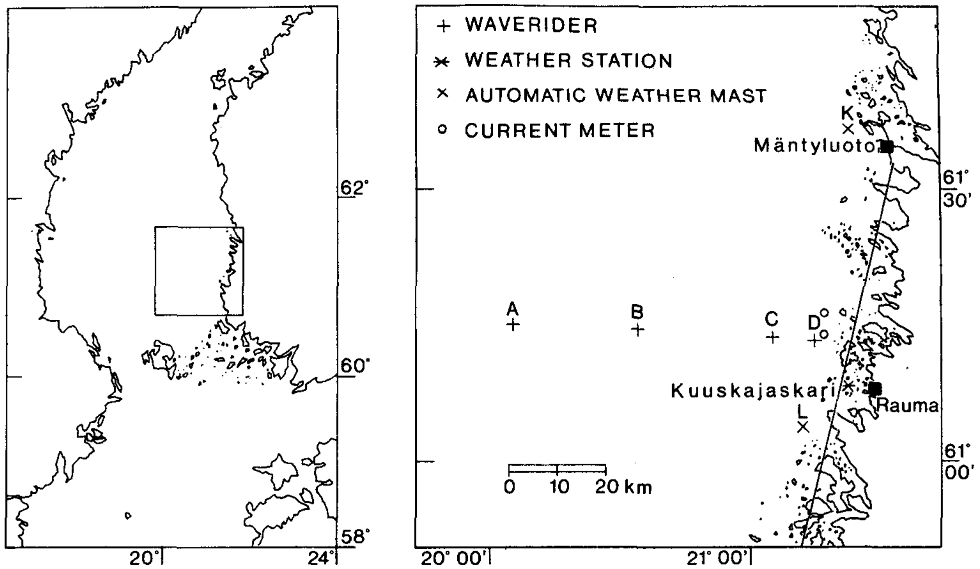

FIG. 1. Location of the wave-profiling line. The straight-line approximation for the shoreline was determined by the least-squares method. The measuring points in the 1979 experiment are close to the points C and D, see Fig. 2.

conditions. An additional experiment was made in 1979, in which only one buoy was used but at different positions.

The wave measuring equipment consisted of Datawell Waverider buoys. The recording and digitizing system resembles that described by Wilson (1975). The measurements began at points C and D in May and the whole system was operating between September and December 1976. Data were collected at intervals of 3 h for 15 min from each buoy. Unfortunately, buoy A was so far from the receiver at Kuuskajaskari Weather Station that a proper registration could be obtained only under the best radio conditions.

Between 24 August and 23 October 1976 the wind was measured at two small flat islets (points K and L, Fig. 1) by automatic weather masts (*Aanderaa*). These masts measured the wind speed and direction at 10 m altitude and the air temperature at 2 m altitude every 15 min. Unfortunately, the data logger at point K malfunctioned and no reliable wind speed data were obtained there. During the 1979 experiment the wind was measured on board R.V. *Aranda* and at point L. The wind was measured also at Kuuskajaskari Weather Station and at Mäntyluoto pilot station. In addition to these measurements, there were available sea-wind estimates at 12 h intervals given out by the Finnish Meteorological Institute.

The wind measuring points at Kuuskajaskari and Mäntyluoto are so close to the shore that in offshore winds they give a poor representation of the conditions in the open sea. Therefore, they were used only as controls.

Data from two current meters (Fig. 1) were available during the best offshore situation in October 1976. Other more extensive current studies have been carried out in the area (Alenius and Mälkki, 1978), partly simultaneously with the wave measurements, but unfortunately not during the best offshore winds.

Because the shoreline is irregular, the average shoreline was approximated by a least-squares straight line. The uncertainty caused by sheltering islands was estimated to be less than ± 1 km. If the sheltering by islands is neglected altogether (which clearly must be unrealistic), the average shoreline ought to be shifted only 2 km inland from the position in Fig. 1.

The bottom depth is shown in Fig. 2. At a depth $h = \pi g/(2\omega^2)$ corresponding to $h = \lambda/4$, a wave component of frequency ω begins to be considerably influenced by the bottom. For ω_m this depth is given by the upper continuous line; the frequency ω_m was calculated from Eq (2) at 25 m s^{-1} offshore wind speed. As the greatest offshore wind speed during the measurements was 13 m s^{-1} (17 m s^{-1} according to the sea-wind estimate) the depth could be regarded as effectively infinite.

On account of the limited data-processing resources available for this study, only a small fraction of the measured spectra were digitized. In choosing the situations for analysis, the first criterion was that the offshore wind had been blowing for at least 24 h. The second criterion was a very small probability of swell in the profile area, as estimated from the history of wind direction on the basis of the weather maps. Only those situations

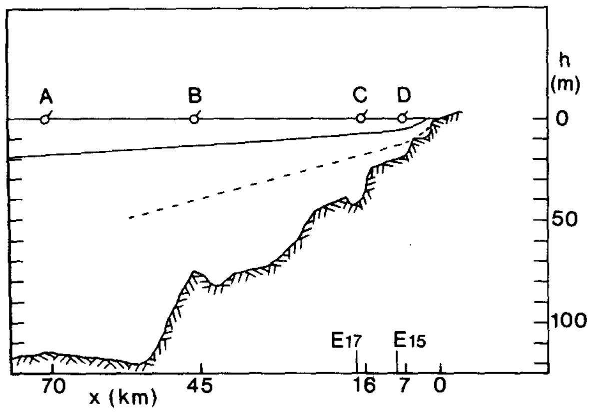

FIG. 2. The bottom topography along the profile. The solid line is the depth $\lambda/4$ at which the influence of the bottom begins to be considerable; the dashed line the depth 0.6λ at which the bottom has almost no influence. The wavelength λ was calculated from (2) using a wind speed 25 m s^{-1}.

in which the weather mast L was operating were accepted for this study.

The best conditions occurred during the period from 11 to 19 October 1976, when a high-pressure cell moved slowly from the northern part of Finland to southeast of Lake Ladoga and caused a wind turning slowly from 40 to 140°. The variations in the 15 min averages of wind speed were sometimes very small (less than ±5% of the long-time averages).

The history of the wind at point L is shown in Fig. 3; the weather map in Fig. 4. The air-sea temperature difference was negative all the time (Fig. 5) and the stratification unstable (bulk Richardson number −0.04 to −0.07).

The conditions during the 1979 experiment were somewhat similar to those in the best period in 1976. A high-pressure cell caused a cold offshore wind onto the measuring area. The stratification was about the same (bulk Richardson number −0.05 to −0.09), but the wind speed was lower (5–8 m s^{-1}),

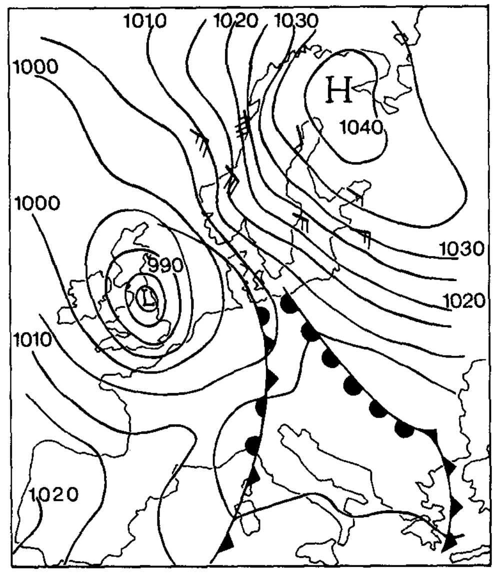

FIG. 4. Weather map for 15 October 1976, 0800 (according to the Finnish Meteorological Institute).

and there were only a few sufficiently long periods of steady wind. This time the wave measurements were made with one buoy that was moved by R.V. *Aranda* to different positions along the observation line.

For the analysis the different generation cases were divided into periods during which the 15 min averages of the wind did not vary more than ±18% in speed and ±20° in direction. The average over such a period was used as a wind parameter. A spectrum was accepted if the wind fulfilled these conditions for at least the stabilizing time, which was ~1.5 h at point D, 3 h at point C and 6 h at point B.

During the period of offshore wind in October 1976 the spectra were found to change in shape with time. At the beginning of the period the spectra had

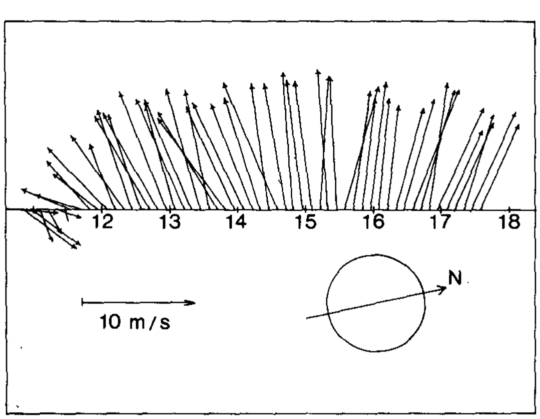

FIG. 3. The history of the wind from 11 to 18 October 1976 as measured by the weather mast at point L.

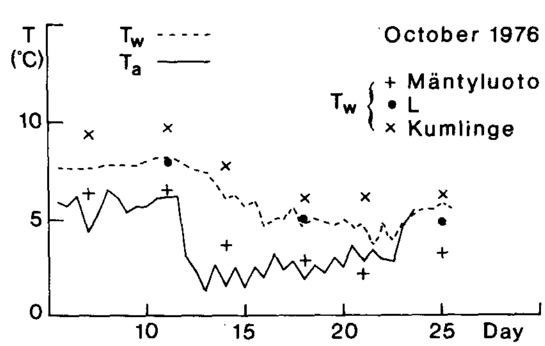

FIG. 5. Temperature conditions in the study area. Water temperature was measured at 15 min intervals by a temperature sensor in the current meter; for comparison surface water temperature is given at point L, at Mäntyluoto 45 km to the north, and at Kumlinge 90 km to the south from point L. Air temperature was measured at point L.

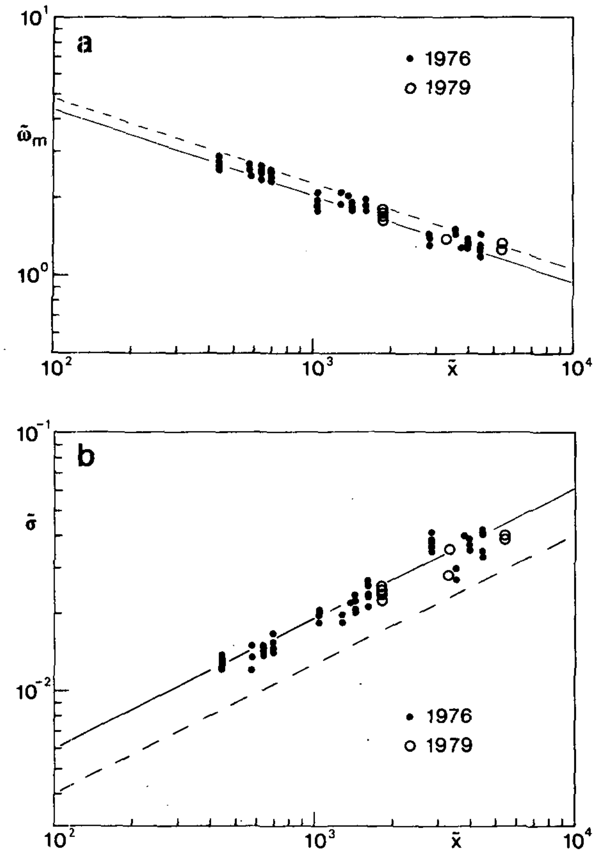

FIG. 6. Dimensionless peak frequency $\tilde{\omega}_m = \omega_m U_{10}/g$, and dimensionless standard deviation of the surface displacement $\tilde{\sigma} = g\sigma/U_{10}^2$ versus dimensionless fetch $\tilde{X} = gX/U_{10}^2$. Solid lines are based on Eqs. (2) and (3); dashed lines on Eqs. (4) and (5) (JONSWAP).

only one significant peak, while at the end a two-peak structure appeared. In this paper we concentrate on single-peaked spectra in the period from 0100 on 13 October to 2000 EET 15 October. During this period the steep forward face of the peak was not disturbed by a low-frequency peak. The two-peaked spectra are discussed by Kahma (1979, 1981a).

3. Results

a. Relations for wave parameters $\tilde{\omega}_m$ and $\tilde{\sigma}$ in terms of $\tilde{X}$

Near the peak the development and the shape of the spectrum were very similar to those observed, for example, in the JONSWAP experiment. The fetch dependence of the parameters $\tilde{\omega}_m$ and $\tilde{\sigma}$ (Fig. 6) shows that the scaling law was clearly valid and we found the following relations:

$$\tilde{\omega}_m = 20\tilde{X}^{-1/3}, \quad (2)$$

$$\tilde{\sigma} = 6 \times 10^{-4}\tilde{X}^{1/2}. \quad (3)$$

The corresponding JONSWAP relations are

$$\tilde{\omega}_m = 22\tilde{X}^{-0.33}, \quad (4)$$

$$\tilde{\sigma} = 4 \times 10^{-4}\tilde{X}^{1/2}. \quad (5)$$

The JONSWAP relation (4) has been determined from a composite data set, which includes also laboratory-scale data. The close agreement between the exponents in (2) and (4) therefore is of interest. They both differ considerably from the $-1/4$ given by Phillips (1977), who used the same composite data set from which (4) was derived, but excluded the laboratory-range observations.

The cause of the exponent $-1/4$ of Phillips mostly seems to lie in the data of Kitaigorodskii and Strekalov (1962), which represent waves near the fully developed stage, and therefore belong to a different population (cf. Fig. 4.17 of Phillips, 1977).

Although the relations (2) and (4) and the exponents in (3) and (5) agree well, the energy predicted by (3) is more than twice that predicted by (5). Various possible sources of error in our measurements were looked into, and it was found that they could not explain the observed difference. Our waveriders were calibrated in the laboratory by hanging them from the rubber cord used for the mooring. The errors in σ were less than the 3% specified by the manufacturer. In addition, a comparison between the waverider and a wave pole was made in 1972. The differences between the waverider and the wave pole lay within the statistical variability.

The wind parameter in our data was measured at point L, which is sufficiently far from the shore that during offshore winds the wind speed should be close to that in the open sea. In neutral stability the wind at 10 m height should reach the open sea value in 2–3 km (Rao *et al.*, 1974; Pasquill, 1972). The wind sensors were calibrated after the experiments; the largest errors found were <2% (Joffre, personal communication). Fig. 2 shows that the finite depth is also clearly excluded as an explanation.

The scattering in Fig. 6 is small, even compared with the JONSWAP data, which were measured in well-defined conditions. This does not support instrumental errors other than of a scaling type.

Several attempts were made to fit the parameters U_{10} and X so as to make the observed growth agree with the JONSWAP relations (4) and (5). The results were mostly quite unrealistic: For example, if both U_{10} and X are determined simultaneously from (4) and (5) using the observed ω_m and σ, the wind is on the average about twice the observed value, i.e., considerably more than the geostrophic wind. The possibility that the effective fetch in the case of an irregular shoreline could be longer than the average fetch clearly is not sufficient. If this were the explanation, the approximate straight shoreline ought to be shifted ~15 km inland before the observed values would on an average agree with the JONSWAP relation (5), and this distance is several kilometers more than the longest bays. In addition, the scaling law was less well obeyed when the estimated shoreline was shifted even slightly. The conclusion, therefore, is that at least a part of the more rapid growth of the waves in our experiment is a real effect and is not related to inaccurate determinations of U_{10} and X.

The difference in the energy is minimized (to ~30%) by assuming that the scaling wind in our experiment should be 1.3 times the observed wind. The systematically higher values of the sea-wind estimates (Fig. 7) lent some support to the possibility that the wind speed at point L was not representative of the wind speed at the measurement line. The new experiment of 1979, however, does not support this explanation. In this latter experiment careful wind measurements were made (in addition to point L) on the R.V. *Aranda*, ~0.5 km from the wave-measuring place. Both an anemometer and very low-flying pilot balloons were used. The anemometer, which was specially installed for this experiment on a 10-m bowsprit on the R.V. *Aranda*, was compared with weather masts on two small islets (Kahma and Leppäranta, 1981); the bias was <2%. In addition, it was found during the calibrations that in offshore wind conditions comparable to those in October 1976 the maximum difference between the wind at point L and on the wave-measuring line was 1 m s^{-1}, and the bias was only 5%. Fig. 6 shows that the new measurements agree with our previous results, but disagree with JONSWAP.

The explanation of the difference may be in external parameters which are not included in the scaling law. The influence of the atmospheric stratification may be significant. Our data were measured in unstable stratification, the JONSWAP data mainly in stable stratification. This explanation is supported by recent measurements by Liu and Ross (1980), who found more rapid growth of waves for unstable stratification than for stable stratification. A further study (Kahma, 1981b) shows, however, that large differences that are correlated with the atmospheric stability occur between data sets that belong to different experiments and that therefore may have other differences in addition to the atmospheric stratification.

b. The saturation range

The well-known Phillips law for the saturation range of the wave spectrum (Phillips, 1958) is based on the assumption that at frequencies substantially above ω_m the spectrum is independent of the wind speed and the fetch. Eq. (1) reduces then to

$$\tilde{S}(\tilde{\omega}, \tilde{X}) = \alpha = \text{constant} \qquad (6)$$

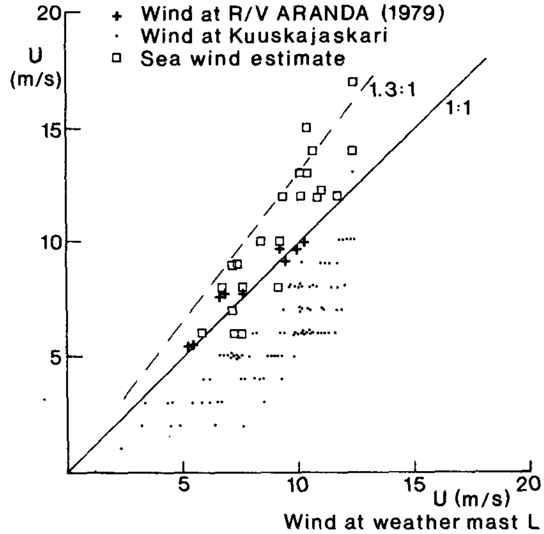

FIG. 7. Wind-speed data from different sources as functions of the wind speed at point L in offshore winds (October 1976 and 1979). The measurements on R/V *Aranda* were made in the wave-profiling area, 20 km to the north from point L.

or, in the case of the wavenumber spectrum $F(\mathbf{k})$,

$$\tilde{F}(\tilde{k}, \varphi, \tilde{X}) = (s(\varphi))^{-1}k^{-4}F(\mathbf{k}) = B = \text{constant}. \qquad (7)$$

Here $\mathbf{k}$ is the wavenumber vector, $\tilde{k} = kU_\infty^2/g$ and $S(\varphi)$ is the spreading factor which satisfies the normalization condition

$$\int_{-\pi}^{\pi} s(\varphi)d\varphi = 1.$$

In the following we use (e.g., Kitaigorodskii, 1970)

$$s(\varphi) = \begin{cases} \dfrac{8}{3\pi}\cos^4\varphi, & |\varphi| < \pi/2 \\ 0, & |\varphi| \geq \pi/2. \end{cases} \qquad (8)$$

When our spectra are presented in the dimensionless form (1), $\tilde{S}(\tilde{\omega}, \tilde{X})$ is found to be independent of $\tilde{X}$ when $\tilde{\omega}$ is fixed, and clearly dependent on $\tilde{\omega}$ when $\tilde{X}$ is fixed (Figs. 8 and 9). In our data $\tilde{S}$ does not show any tendency to approach a constant value with increasing $\tilde{\omega}$ (the spectrum above 0.5 Hz is not used in the dimensionless presentation). An individual spectrum, therefore, does not follow the -5 power law $[S(\omega) = \alpha g^2\omega^{-5}]$ of Eq. (6), at least when $\omega < 4$.

The accuracy of the waverider has been verified for frequencies <0.5 Hz in several intercalibrations (e.g., Hasselmann *et al.*, 1973; Donelan, 1978). Above 0.5 Hz the transfer function of the 0.7 m diameter buoy begins to rise. A good agreement was found in our comparison measurements between the waverider buoy and a wave pole even up to 0.8 Hz (Kahma, 1981a) when the transfer function

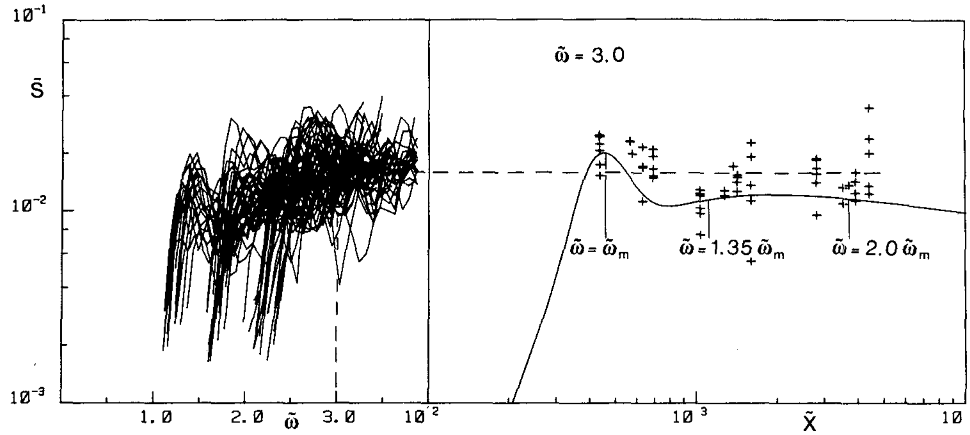

FIG. 8. The measured dimensionless spectra $S(\tilde{\omega}, \tilde{X})$ as functions of $\tilde{\omega} = U_{10}\omega/g$ at all fetches on the left, and the value of $\tilde{S}$ at $\tilde{\omega} = 3.0$ as a function of $\tilde{X} = gX/U_{10}^2$ on the right. The solid line on the right is the JONSWAP spectrum as a function of $\tilde{X}$ at $\tilde{\omega} = 3.0$. For three points the fixed value $\tilde{\omega} = 3.0$ is given as a fraction of $\tilde{\omega}_m(\tilde{X})$, the peak frequency of the JONSWAP spectrum. The average spectra are shown in Fig. 9.

was used to correct the spectrum from the waverider (the new models of the receiving unit are provided with a 0.6-Hz low-pass filter, but this filter was not installed in the unit used in the present study). Recent laboratory calibrations in a wave tank indicate, however, that this agreement probably was accidental above 0.6 Hz.

Several authors (Hasselmann *et al.*, 1973; Mitsuyasu, 1969; Longuet-Higgins, 1969) have found that α is not constant but depends on the dimensionless fetch. Although this seems to contradict our results, we want to show that it does not necessarily mean that their data would not lead to the same results as ours, if presented in form (1).

There are slightly different methods for determining α. The standard method is to take the mean of $\tilde{S}$ over a frequency band sufficiently far above ω_m. In the JONSWAP data α was defined as a mean of $S(\omega)\omega^5 g^{-2} \times \Phi_J^{-1}$, where

$$\Phi_J = \exp\left\{-\frac{5}{4}\left(\frac{\omega_m}{\omega}\right)^4 + \ln\gamma_J \times \exp\left[\frac{-(\omega - \omega_m)^2}{2\delta^2\omega_m^2}\right]\right\}$$

is the shape function of the JONSWAP spectrum (Hasselmann *et al.*, 1976). The mean was taken in the frequency range $1.35\omega_m < \omega < 2\omega_m$, where the dimensionless shape parameters δ and γ_J (mean JONSWAP values $\gamma_J = 3.3$, $\delta = 0.07$, $\omega < \omega_m$; $\delta = 0.09$, $\omega > \omega_m$) have no influence. To avoid confusion we hereafter refer to this parameter as α_J.

Fig. 10 shows α_J from our data as a function of the dimensionless fetch $\tilde{X}$. For a comparison, the JONSWAP data are added to the figure. The general dependence on the dimensionless fetch $\tilde{X}$ is very similar. Our data show slightly higher values at the same $\tilde{X}$, in agreement with the difference between (3) and (5).

The dependence of α_J on $\tilde{X}$ seems therefore to be a consequence of the combined effect of a deviation from the -5 power law, the relation between $\tilde{X}$ and the averaging frequency band $1.35\omega_m < \omega < 2\omega_m$, and the shape function Φ_J.

Fig. 8 also shows that, as a function of $\tilde{X}$, the dimensionless spectrum $\tilde{S}_J = S_J\omega^5 g^{-2}$, where S_J the JONSWAP spectrum,

$$S_J(\omega) = g^2\omega^{-5}\alpha_J\Phi_J(\omega),$$

is practically constant in the range $1.35\omega_m < \omega < 2\omega_m$. On the other hand, Fig. 9 shows that the observed dependence of $\tilde{S}(\tilde{\omega}, \tilde{X})$ on $\tilde{\omega}$ is described by $\tilde{S}_J$, when $\omega < 2\omega_m$.

The JONSWAP spectrum is therefore a good approximation for the frequencies near the peak. This

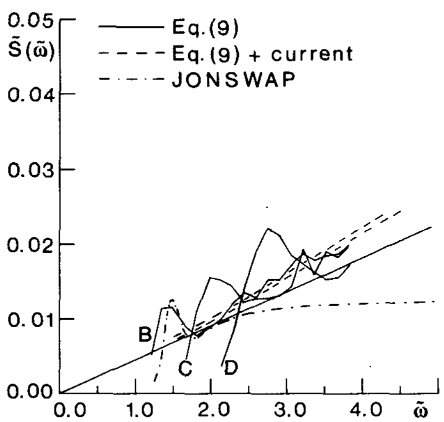

FIG. 9. Averages of the dimensionless spectra in Fig. 8 on a linear scale. The letters *B*, *C*, *D* refer to different wave buoys. The dot-dashed line is the JONSWAP spectrum with $\tilde{\omega}_m = 1.5$. The straight solid line is Eq. (9), and the short dashed lines Eq. (9) plus the effect of the 0.3 and 0.4 m s^{-1} currents.

also explains why in a suitable fixed frequency band (not too far from the peak) it was possible in our data to obtain the dependence of α_J on $\tilde{X}$. When the standard α was calculated from the same fixed frequency band, there was no dependence on the fetch.

Our next step is to discuss the possible reasons for this deviation from the Phillips -5 power law. Kitaigorodskii *et al.* (1975) have pointed out several factors that may alter the frequency spectrum although the wavenumber spectrum still has the form (7). Such factors are finite depth, permanent currents and the presence of long-wave components.

The influence of the finite depth h on the frequency spectrum disappears nearly completely when $\omega(h/g)^{1/2} > 2$ (Kitaigorodskii *et al.*, 1975). Fig. 2 shows the depth $h = 4g/\omega_m^2$, where ω_m is determined from Eq. (2) at 25 m s^{-1} wind speed. Clearly, the waves are generated in deep water also in this respect and we can exclude the finite depth as an explanation. In addition, no significant swell components were present in this set of spectra.

The current was measured near the coast using current meters at depths of 7 and 8 m (about half of the total depth). The current was steady and ~0.3 m s^{-1} toward the south. Within 1 km landward from the current meter the depth decreases to 3 or 4 m. The observed direction therefore is quite understandable. The surface current was estimated from this data by a surface drift model (Häkkinen, personal communication) to be about the same strength and toward the west.

It is therefore reasonable to assume, in agreement with the general knowledge of surface currents in steady wind conditions ($v \approx 0.02U_{10}$), that the surface current was ~0.3 m s^{-1} in the direction of the waves.

Using the nomograms of Kitaigorodskii *et al.* (1975) it can be seen that the Doppler effect of the current can explain only a small fraction of the observed deviation from the -5 power law. It is not even possible to find a current speed which could explain the observations.

Using the laboratory data of Shemdin on the dispersion relation in the case of a shear current (Shemdin, 1972; in reparameterized form in Wu, 1975) we calculated that at the frequencies of our data the wind-driven shear current has only a very small additional effect on the Doppler shift caused by a current which is constant with depth.

In the following we shall therefore abandon the assumption that the wavenumber spectrum has the form (7), which is independent of both wind speed and fetch, and study the more general form (1).

Since we already have found that the dimensionless spectrum $\tilde{S}$ is (at least within the accuracy of our data) independent of $\tilde{X}$, the function $\tilde{S}(\tilde{\omega}, \tilde{X})$ is given by the average spectra in Fig. 9. To get more general results, however, we shall first exclude

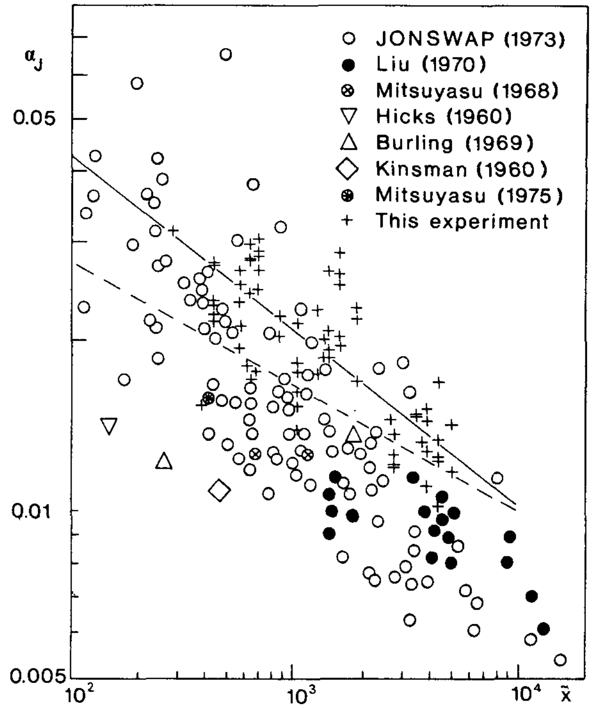

FIG. 10. Parameter α_J determined by the method given by Hasselmann *et al.* (1976). The obvious dependence on $\tilde{X}$ is mainly a consequence of the -4 power law of the spectrum. The data from other sources and the dashed regression line are taken from Hasselmann *et al.* (1973). The continuous regression line represents these data.

the influence of the Doppler effect. In this case the nomograms of Kitaigorodskii *et al.* (1975) cannot be used, since they are derived for the case of Eq. (7). Therefore, we must follow their calculations and solve for the function

$$\tilde{F}(\tilde{k}, \varphi) = F(\mathbf{k})k^4/s(\varphi),$$

which gives the observed $\tilde{S}(\tilde{\omega})$. The relation between the frequency spectrum and the wavenumber spectrum is (Kitaigorodskii *et al.*, 1975),

$$S(\omega) = \int_{-\pi}^{\pi} F(k, \varphi) \frac{k}{G(k, \varphi)}\bigg|_{k=k(\omega,\varphi)} d\varphi,$$

where $k(\omega, \varphi)$ and $G(k, \varphi)$ are defined through the equations

$$\omega_v = \omega v/g,$$

$$y = \omega_v \cos(\varphi - \theta),$$

$$K_v(y) = \left[\frac{(1 + 4y)^{1/2} - 1}{2y}\right]^2,$$

$$f(y) = [K_v(y)]^{1/2} + 2y,$$

$$k = \frac{\omega^2}{g} K_v(y),$$

$$G = \frac{g}{2\omega} f(y),$$

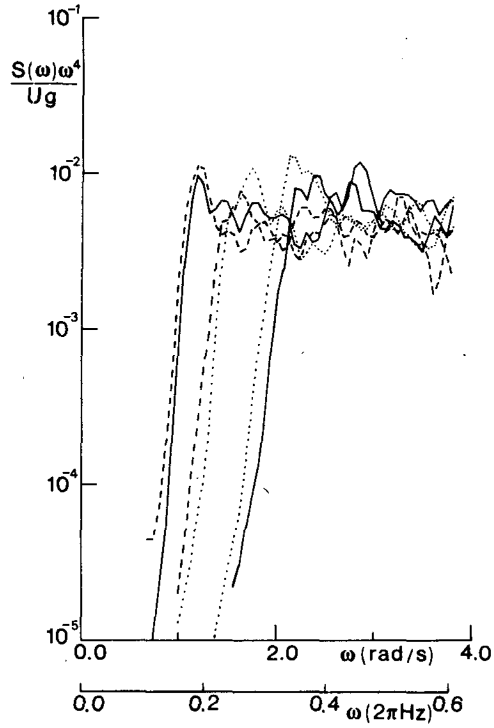

FIG. 11. Examples of spectra presented in the form $S(\omega)\omega^4 g^{-1} U_{10}^{-1}$. Two spectra were chosen randomly from each of the points B, C and D.

and v the current velocity, $\mathbf{k} = (k\cos\varphi,\ k\sin\varphi)$ and $\theta =$ the angle of the current with respect to the wind.

It was found numerically that, if we take as the function $\tilde{F}$ the expression

$$\tilde{F}(\tilde{k},\ \varphi) = B_u \tilde{k}^{1/2} \times S(\varphi),$$

with $B_u = 7.1 \times 10^{-3}$, we obtain a spectrum $\tilde{S}(\tilde{\omega})$ which closely approximates our data (Fig. 9). When there are no currents the corresponding relation in the frequency domain is

$$\tilde{S}(\tilde{\omega}) = \alpha_u \tilde{\omega}, \tag{9}$$

where $\alpha_u = 4.5 \times 10^{-3}$. Eq. (9) can be written in the form

$$S(\omega) = \alpha_u U_{10} g \omega^{-4}, \tag{10}$$

which shows that the spectrum should have a -4 power law.

The effect of the Doppler shift is shown in Fig. 9, when the current speed is 0.3 and 0.4 m s^{-1}, $\theta = 0$ and the spreading function has the form (8). The result is not sensitive to the precise values of the current speed or to the form of the spreading function.

It is clear from Fig. 9 that the influence of the Doppler shift means a relatively small correction to the power law in the saturation range of the spectrum. This is even more evident from Fig. 11, which shows that the deviation from the -4 power law is small.

c. The growth of a wave component

In general, the development of the spectrum with increasing fetch is similar to that observed, for example, in the JONSWAP experiment. The overshooting (first reported by Barnett and Wilkerson, 1967) is clearly seen in almost all of the spectra, and the presentation using Eq. (1) (Fig. 12) shows that the phenomenon is real and is not merely a consequence of the statistical variability of the spectrum combined with a free choice of ω_m. The spectral density

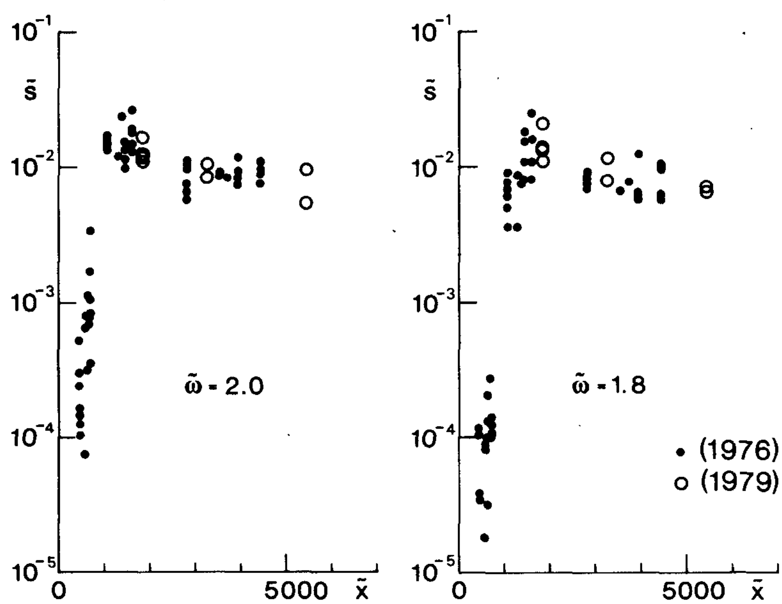

FIG. 12. The growth of the dimensionless spectrum $\tilde{S} = S\omega^5 g^{-2}$ with dimensionless fetch $\tilde{X} = gX/U_{10}^2$ at fixed $\tilde{\omega} = U_{10}\omega/g$.

at the peak is in this data 2.0 times that predicted by Eq. (9), and no dependence on $\tilde{\omega}$ can be seen.

The approximately exponential growth reported by Snyder and Cox (1966), Barnett and Wilkerson (1967) and Mitsuyasu and Rikishi (1978) also is observed in our data at fixed $\tilde{\omega}$ (Fig. 12).

To calculate the dimensionless growth rate β

$$\beta = \frac{1}{\omega S(\omega)} \frac{\partial S(\omega)}{\partial t},$$

$(\ln\tilde{S})/\Delta\tilde{X}$ was determined by a least-squares fit. The relation between fetch and time was calculated assuming, as usual (e.g., Mitsuyasu and Rikiishi, 1978), $X = c_g t$, where the group velocity is

$$c_g = \int_{-\pi}^{\pi} s(\varphi) \frac{g}{2\omega} \cos\varphi d\varphi = \frac{0.91g}{2\omega},$$

when Eq. (8) is used for the spreading factor. The growth rate was then found from the equation

$$\beta = \frac{\Delta \ln\tilde{S}}{\Delta\tilde{X}} \times 0.46\tilde{\omega}^{-2}.$$

Fig. 13 shows $2\pi\beta$ as a function of $\tilde{\omega} = U_{10}/c$. The data from other sources are taken from DeLeonibus and Simpson (1972). The growth rates observed in our data are in good agreement with previous observations when $\tilde{\omega} < 2$. Above $\tilde{\omega} = 2$ the fetch range from which the growth rate is determined in our data becomes very short.

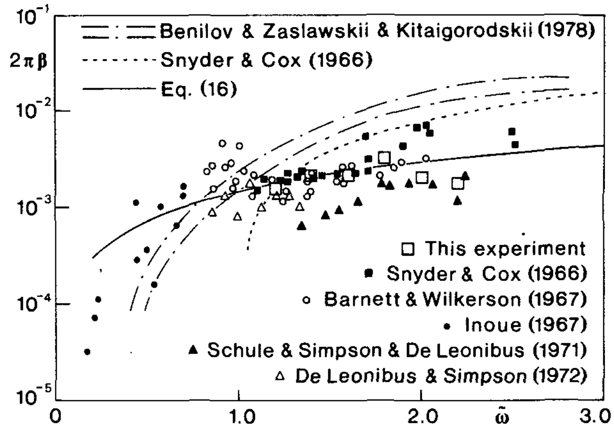

FIG. 13. The dimensionless growth rate parameter $2\pi\beta$ versus $\tilde{\omega} = U_{10}/c$. The data from other sources were taken from DeLeonibus and Simpson (1972); $C_{10} = 1.3 \times 10^{-3}$ was used to convert u_*/c to U_{10}/c. The solid line [Eq. (16)] is calculated from the model discussed in Section 4b.

4. Discussion

a. The saturation range

Although the Phillips -5 power law has been assumed in most of the previous works concerning the saturation range of the spectrum, there has been some discussion about the other power laws. Already in 1962 Kitaigorodskii suggested the power law -4 for a certain high-frequency range. However, the derivation was based on the assumption that there exists a frequency range in which the spectrum depends only on the dissipation (or input) of energy and on the frequency. At least in the frequency range in which the -4 power law was observed in our spectra it is clearly not possible to neglect the influence of gravity. It is even doubtful if there exists a frequency range in which both gravity and surface tension can be simultaneously neglected and therefore the theoretical justification of the so called Kitaigorodskii range (Pierson and Stacy, 1973; Bjerkaas and Riedel, 1979) is open. In addition, the lower boundary of the Kitaigorodskii range in the model of Bjerkaas and Riedel is about $\tilde{\omega} = 10$ and therefore the Kitaigorodskii range is not relevant to the frequency range of our data.

In the low-frequency gravity range the -4 power law has been reported by Kawai *et al.* (1977), who found $\alpha_u = 3.2 \times 10^{-3}$. From the composite set of data by Hasselmann *et al.* (1976), Toba (1978) has also derived the relation $\alpha = 7 \times 10^{-3}\omega_m U_{10}/g$, which shows that the data can be interpreted according to Eq. (9). The spectra of Mitsuyasu *et al.* (1980) show also a -4 power law with $\alpha_u = 3.5 \times 10^{-3}$. They also point out that the JONSWAP spectrum follows closely a -4 power law when $\omega_m < \omega < 2\omega_m$.

To test whether the other existing data support the -4 power law, the spectra of Moskowitz (1964) were analyzed. All the synoptically chosen spectra decreased with frequency even more slowly than the -4 power law. The average α_u was found to be 7.2×10^{-3}; however, the limited accuracy of the Tucker shipborne recorder and the fairly large accepted moving velocity (up to ± 1 m s^{-1}) make these data less reliable in this respect.

Longuet-Higgins (1969) has made a semi-theoretical calculation of the saturation range coefficient α for the case when the spectrum has the Phillips form

$$S(\omega) = \begin{cases} \alpha g^2 \omega^{-5}, & \omega > \omega_m \\ 0, & \omega < \omega_m. \end{cases} \tag{11}$$

His basic assumption is that wave breaking occurs when the wave amplitude a exceeds $a_0 = g/2\bar{\omega}^2$, where the mean frequency is

$$\bar{\omega}^2 = \sigma^{-2} \int_0^\infty \omega^2 S(\omega) d\omega.$$

When the wave amplitude exceeds a_0, wave breaking reduces it back to a_0. The mean loss of energy per average cycle $T = 2\pi/\bar{\omega}$ is

$$E_d = \int_{a_0}^\infty \tfrac{1}{2}\rho_w g(a^2 - a_0^2)P(a)da.$$

Using the Rayleigh distribution for $P(a)$ Longuet-Higgins finds that

$$E_d = E_w \exp(-E_0/E_w),$$

where $E_0 = \frac{1}{2}\rho_w g a_0^2$, and

$$E_w = \rho_w g \sigma^2 = \rho_w g \int_0^\infty S(\omega)d\omega.$$

We shall now apply these results to the case when the spectrum has the form

$$S(\omega) = \begin{cases} \alpha_u g U_{10}\omega^{-4}, & \omega > \omega_m \\ 0, & \omega < \omega_m. \end{cases}$$

This gives

$$E_0 = \tfrac{1}{72}\rho_w g^3 \omega_m^{-4}, \quad \bar{\omega} = \sqrt{3}\omega_m,$$

$$E_w = \tfrac{1}{3}\rho_w g^2 \alpha_u U_{10}\omega_m^{-3},$$

and

$$\frac{E_d}{E_w} = \exp\{(-24\alpha_u\tilde{\omega}_m)^{-1}\}, \quad \tilde{\omega}_m = \omega_m U_{10}/g.$$

The energy absorbed by the waves in a mean cycle can be approximated by $\rho_a C_{10} U_{10}^2 \bar{c}\gamma_w T$, where $\bar{c} = g/\bar{\omega}$ is the mean phase speed of the waves, C_{10} the drag coefficient and $\tau_a\gamma_w$ the fraction of the momentum flux τ_a which goes to the waves. At saturation this must be equal to E_d and

$$\frac{E_d}{E_w} = 2\pi \frac{\rho_a}{\rho_w} C_{10}\gamma_w\tilde{\omega}_m\alpha_u^{-1}.$$

For a fully developed sea, we may assume $\tilde{\omega}_m = 0.9-1.0$, $C_{10} = (1.0-1.3) \times 10^{-3}$, $\gamma_w = 0.1-1.0$ and $\rho_a/\rho_w = 1.2 \times 10^{-3}$, which gives $\alpha_u = (4.4-6.4) \times 10^{-3}$.

The values of α_u are summarized below:

Kawai, Okada and Toba (1977)	3.2×10^{-3}
Hasselmann *et al.* (1976)	7.0×10^{-3}
Mitsuyasu *et al.* (1980)	3.5×10^{-3}
Moskowitz (1964)	7.2×10^{-3}
This experiment	4.5×10^{-3}
Calculated (mean)	5.4×10^{-3}
Mean	5.1×10^{-3}

In the following we shall introduce a possible explanation for the wind-speed dependence in the saturation range. For scales considerably larger than the gravity-capillary scale the limiting process of waves is the breaking by whitecaps, which typically occurs when the waves move with their phase speed into a region where the energy (which moves with the group velocity) is locally high. Breaking also occurs when a small wave riding over a longer one has an energy excess as a result of the radiation stress effect (Phillips, 1977). The important feature is that whitecapping is an intermittent phenomenon which takes place only on a small fraction of the surface area. On the rest of the sea surface the waves are considerably below the limiting configuration and may therefore grow.

Three assumptions are as follows:

(i) When a wave breaks by the mechanism of whitecapping, the energy is lost in turbulence and as current in a certain narrow frequency range and is not transferred by strong nonlinearities to other frequency ranges.

(ii) The nonlinear transfer of energy by resonant wave-wave interactions is not important.

(iii) The probability distribution of the heights of the waves in a fixed frequency range is stationary (probably a Rayleigh distribution), when the height scale is normalized by the square root of the energy of the frequency range.

Observations show that the growth rate parameter β is dependent on $\tilde{\omega} = U_{10}/c$. At a fixed frequency this means that an increase of the wind speed increases the growth; under our assumptions this means that the energy input is increased. It is reasonable to assume that the energy input is increased also in the saturation range although the scale may be different compared with the unsaturated forward face of the spectrum.

If the input of energy in a certain frequency band is increased with increasing wind speed, it must be balanced by more breaking in the same band. There are three ways to lose more energy by breaking: whitecaps may occur more frequently, the height of the wave may be greater before breaking, or the energy after breaking may be smaller. A high wind may break a sharp crest slightly below the limiting configuration, but this probably is not important in the first approximation. From our third assumption it follows that, if whitecaps are to occur more frequently, either the energy of the given band must be increased or there must be more influence from external factors, e.g., long waves which appear when the peak of the spectrum moves to lower frequencies. As a result the spectrum in the saturation range can be independent of wind speed only if there is a balance between the influence of external factors and the increase in the wind speed, which is unlikely. Accordingly, without giving up the assumption that the limiting configuration of breaking waves is independent both of the fetch and the wind speed, the saturation range of the spectrum may under these assumptions still be dependent on the wind speed. The above reasoning is valid only for frequency ranges in which the breaking occurs as whitecapping and depends, as a first approximation, on the energy of the breaking frequency band only. On the smaller scale, in which the surface drift layer becomes important, the dissipation takes place as microscale breaking (Phillips and Banner, 1974). In this case the breaking occurs substantially before the crest becomes sharp. In this range also the influence of longer waves may become significant. We may therefore not expect that the form (9) would hold with constant α_u for the entire high-frequency range.

It has been reported by several authors (Pierson and Stacy, 1973; Toba, 1973; Mitsuyasu, 1977) that in the capillary-gravity range the spectrum has the form

$$S(\omega) = \alpha_* u_* g_* \omega^{-4},$$

where $g_* = g + \gamma k^2$, and λ is the ratio of surface tension to water density. Toba (1973) has derived this equation from his $-3/2$ power law of individual waves and suggests that it should hold for the entire saturation range. The constant α_*, however, is considerably smaller than $\alpha_u C_{10}^{-1/2}$ in the gravity range. Therefore, as pointed out also by Mitsuyasu *et al.* (1980), there may exist a range in which the spectrum must decrease more rapidly with frequency than ω^{-4}. This may explain the evident -5 power law in the data of Burling (1959) and in the 1–4 Hz range in the data of Mitsuyasu (1977).

Phillips (1978) has suggested an explanation for the -4 power law for the very high frequency part of the saturation range. According to him, the occurrence of isolated irregular line segments across which the slope changes by an amount Δf is associated with a frequency spectrum of slope which has a -2 power law. In the case of non-dispersive waves he obtains

$$S(\omega) \sim u_* g \overline{(\Delta f)^2} \omega^{-4}.$$

In the range $\tilde{\omega} < 4$ in which the -4 power law was observed in our data the waves probably are almost dispersive and therefore it does not seem likely that this explanation can be extended to the range of our data.

If we assume that the influence of the surface drift layer is connected with the transition from the -4 power law to the -5 power law we may get an estimate of the possible transition frequency $\tilde{\omega}_\alpha$. According to Phillips (1977), the breaking should occur by the collapse of essentially irrotational waves, when the phase speed of the waves is at least 5–10 times larger than the velocity difference across the surface drift layer. According to Wu (1975) this velocity difference is $\sim 0.55 u_*$, which gives an estimate of about 5–10 for $\tilde{\omega}_\alpha$. It is interesting to note that in the spectrum of Mitsuyasu (1977) there is a short range between $\omega_m/2\pi = 0.75$ and 1 Hz in which the spectrum has a -4 power law. The wind speed $U_{10.5}$ was 8 m s^{-1} in the data of Mitsuyasu, which means $\tilde{\omega}_\alpha \approx 5$. In the data of Burling (1959) there seems to be no -4 power law above the highest peak frequency $\tilde{\omega}_m \approx 6$, but the spectral densities of the peaks $S(\omega_m)$ show (in spite of a considerable scatter) a dependence on $\tilde{\omega}$ and therefore do not contradict the -4 power law; this also gives $\tilde{\omega}_\alpha$ about 5.

The -4 power law in the spectrum of Mitsuyasu (1977), of course, may be equally well an undershooting effect; however, the undershooting is then stronger than our data show (cf. Fig. 11). The support for the -4 power law when $\tilde{\omega} < 5$ is also weak in the data of Burling (1959). Our data in Figs. 9 and 11 do not extend to the possible transition frequency. If the frequencies above 0.5 Hz are used the data do not show any tendency to approach the -5 power law, but, as already mentioned by Kahma (1981a) the accuracy of the buoy is perhaps not sufficient at frequencies above about 0.6 Hz. Recently, in discussing the possible reasons for the deviations from the Phillips -5 power law Kitaigorodskii (1981) presents duration-limited spectra which near the peak follow the -5 power law fairly closely, but at higher frequencies (still in the gravity range) show dependence on the wind and a power law near -3.5. This contradicts the transition mentioned in the above but, on the other hand, it has been shown (Kitaigorodskii, 1970; Mitsuyasu and Rikiishi, 1978) that there is not a complete correspondence between duration-limited and fetch-limited waves.

In summary, the data do not exclude the possibility that for fetch limited waves at $\tilde{\omega}_\alpha \approx 5$ there would be a transition from the -4 power law to the -5 power law. However, more data are needed before conclusive results can be reached.

b. The growth rate

Assuming the form of the wave spectrum, a relation can be found between that fraction of the momentum transferred from the atmosphere which remains in waves, and the growth-rate parameter β. Such calculations have recently been carried out in the case of the Phillips spectrum (11) (Benilov *et al.*, 1978b) and the JONSWAP spectrum with constant α (Benilov *et al.*, 1978a).

To study the case when the high-frequency part of the spectrum has the form (10), we write the energy and momentum of the waves in the form

$$E_w = \rho_w g \int_0^\infty S(\omega) d\omega = \frac{r_E}{3} \rho_w g^2 \alpha_u U_{10} \omega_m^{-3},$$

$$M_w = \rho_w \int_0^\infty \omega S(\omega) d\omega = \frac{r_M}{2} \rho_w g \alpha_u U_{10} \omega_m^{-2},$$

where r_E and r_M are parameters which roughly describe the contribution of the overshooting part and the forward face of the spectrum. In addition, we define

$$r_g = E_w^{-1} \rho_w g \int_0^{\omega_m} S(\omega) d\omega,$$

$$\omega_g^2 = \frac{\rho_w g}{r_g E_w} \int_0^{\omega_m} \omega^2 S(\omega) d\omega.$$

Parameters r_E, r_M, r_g and ω_g/ω_m may be approximated by constants which, according to our data and the JONSWAP spectrum $S_J(\omega)$, are $r_E \approx r_M \approx 2$, $r_g \approx 0.3$ and $\omega_g \approx 0.9\omega_m$.

The net increase in energy and momentum can now be written

$$\frac{\partial E_w}{\partial t} = -r_E \rho_w g^2 \alpha_u U_{10} \omega_m^{-4} \frac{\partial \omega_m}{\partial t}, \quad (12)$$

$$\frac{\partial M_w}{\partial t} = -r_M \rho_w g \alpha_u U_{10} \omega_m^{-3} \frac{\partial \omega_m}{\partial t}. \quad (13)$$

On the other hand,

$$\frac{\partial M_w}{\partial t} = \tau_n = \gamma_n \rho_a C_{10} U_{10}^2, \quad (14)$$

where $\gamma_n = \tau_n/\tau_a$ (τ_a is the wind stress and τ_n the fraction which remains in the waves).

We shall now assume that the nonlinear transfer by the wave-wave interactions is not the main factor in the growth of a wave component. Because the forward face of the spectrum is steep and rises approximately exponentially with ωt, and since only the unsaturated part of the spectrum contributes under these assumptions to the net growth, we may approximate

$$\beta = \frac{1}{\omega_g E_w r_g} \frac{\partial E_w}{\partial t}. \quad (15)$$

From (12)–(15), we get

$$\beta = \frac{C_{10}\gamma_n}{\alpha_u} \frac{\rho_a}{\rho_w} \frac{U_{10}}{c} \frac{3}{r_M r_g (\omega_g/\omega_m)^2}, \quad (16)$$

where $c = g/\omega_g$. Fig. 13 shows that if we take $C_{10}\gamma_n = 1.4 \times 10^{-4}$ (Donelan, 1978), $\alpha_u = 4.5 \times 10^{-3}$ and $\rho_a/\rho_w = 1.2 \times 10^{-3}$, (16) agrees well with the observations, even better than the empirical equation

$$\beta = \frac{\rho_a}{\rho_w}\left(\frac{U_{10}}{c} - 1\right) \quad (17)$$

of Snyder and Cox (1966).

Snyder and Cox (1966) have shown that, if (17) holds for the whole spectrum (11), the momentum flux to fully developed waves would be about an order of magnitude greater than the total stress τ_a. Hasselmann *et al.* (1973) explained this paradox by nonlinear wave interactions. To check whether the paradox still exists if (16) is used, we approximate the high frequency part of the spectrum by

$$\tilde{S}(\tilde{\omega}) = \begin{cases} \alpha_u \tilde{\omega}, & \tilde{\omega}_m < \tilde{\omega} < \tilde{\omega}_\alpha \\ \alpha_u \tilde{\omega}_\alpha, & \tilde{\omega}_\alpha < \tilde{\omega}, \end{cases}$$

where $\tilde{\omega}_m \approx 0.9$, $\tilde{\omega}_\alpha \approx 5$ (cf. Section 4a). If we take into account that when the waves can grow, $\beta\omega S = \partial S/\partial t$, and assume that the momentum flux to a wave component in the saturated part of the spectrum depends on the value of the spectral component in the same way as in the unsaturated part, then the momentum flux to fully developed waves is

$$\tau_w = \rho_w \int_{\omega_m}^{\infty} \omega\beta\omega S(\omega) d\omega.$$

Assuming that γ_n in (16) is a constant when $\omega > \omega_m$ we get

$$\tau_w = \rho_a C_{10} U_{10}^2 \gamma_n \left(\ln \frac{\omega_\alpha}{\omega_m} + 1\right) \frac{3}{r_M r_g (\omega_g/\omega_m)^2}$$
$$= \tau_a \nu_n R,$$

where $R \approx 16$. This gives $\gamma_n < 0.063$, which is in agreement with the observed γ_n (Donelan, 1978) when the waves are relatively well developed. The result, however, means that a very large fraction (from 50 to 100%) of the momentum flux from the atmosphere should go to the waves from which it is then transformed into turbulence and current.

5. Conclusions

The development of the wave spectrum with fetch in steady wind conditions was studied with a line of consecutive wave buoys. Data were obtained from a period of exceptionally steady offshore wind. The relationship between dimensionless peak frequency $\tilde{\omega}_m$ ($=\omega_m U_{10}/g$) and dimensionless fetch $\tilde{X}$ ($=gX/U_{10}^2$) was close to that of previous observations. The relationship between dimensionless energy $\tilde{\sigma}^2$ ($=g^2\sigma^2/U_{10}^4$) and $\tilde{X}$ was linear, as previously observed, but the energy was approximately twice that reported in the JONSWAP experiment. Various possible sources of error in our measurements were looked into and it was concluded that at least a considerable part of this difference must be real. External parameters which are not included in the scaling law, such as atmospheric stratification, might be the reason for this difference.

In the saturation range the dimensionless spectrum showed a clear deviation from the Phillips -5 power law. The dimensionless spectrum was practically independent of $\tilde{X}$ and had (when the Doppler effect by the current was excluded) the form $S(\omega)\omega^5 g^{-2} = \alpha_u \tilde{\omega}$, at least when $\tilde{\omega} < 4$, which means that the spectrum in the saturation range is dependent on the wind speed and has a -4 power law. The constant α_u was estimated from our data to be 4.5×10^{-3}. The properties of our spectra are satisfactorily described by the JONSWAP spectrum, when $\omega < 2\omega_m$. Above $2\omega_m$ the JONSWAP spectrum approaches the -5 power law; this type of behavior was not observed in our spectra.

The theoretical method of Longuet-Higgins (1969) to estimate the Phillips saturation-range constant α is applied to estimate α_u. The result $\alpha_u = (4.4–6.4) \times 10^{-3}$ agreed well with the observed α_u. A qualitative explanation for the dependence of the spectrum on the wind speed in the saturation range is proposed.

The growth of a component of the dimensionless spectrum with $\tilde{X}$ was found to be exponential within the accuracy of the data. The exponential-growth parameter β agreed well with previous observations. When the spectral form (10) is applied to our modification of the model of Benilov *et al.* (1978a), an equation for the growth-rate parameter is obtained which agrees very well with observations.

Acknowledgments. I am indebted to Prof. S. A. Kitaigorodskii for his inspiring lectures and helpful discussions. I am grateful to Dr. F. Dobson, Dr. M. Donelan, Dr. J. Elliott, Dr. P. Mälkki, and Dr. S. Smith for valuable discussions. I further wish to thank Mr. J. Holmström of the Shipbuilding Laboratory of the Helsinki University of Technology, and the National Board of Public Roads and Waterways for their cooperation in the field experiments.

REFERENCES

Alenius, P., and P. Mälkki, 1978: Some results from the current measurement project of the Pori-Rauma region. *Finn. Mar. Res.*, **244**, 52–63.

Barnett, T. P., and J. C. Wilkerson, 1967: On the generation of ocean wind waves as inferred from airborne radar measurements of fetch limited spectra. *J. Mar. Res.*, **25**, 292–321.

Benilov, A. Yu., M. M. Zaslavskii and S. A. Kitaigorodskii, 1978a: Construction of small-parameter models of wind wave generation. *Oceanology*, **18**, 387–390.

——, A. I. Gumbatov, M. M. Zaslavskii and S. A. Kitaigorodskii, 1978b: A nonstationary model of development of the turbulent boundary layer over the sea with generation of surface waves. *Izv. Akad. Nauk, SSSR, Atmos. Ocean Phys.*, **14**, 830–836.

Bjerkaas, A. W., and F. W. Riedel, 1979: Proposed model for the elevation spectrum of a wind-roughened sea surface. The Johns Hopkins University, APL TG 1328 1-31, 31 pp.

Burling, R. W., 1959: The spectrum of waves at short fetches. *Dtsch. Hydrogr. Z.*, **12**, 45–64, 96–117.

DeLeonibus, P. S., and L. S. Simpson, 1972: Case study of duration-limited wave spectra observed at an open ocean tower. *J. Geophys. Res.*, **77**, 4555–4569.

Donelan, M., 1978: On the fraction of wind momentum retained by waves. *Marine Forecasting*, J. C. J. Nihoul, Ed., Elsevier, 141–159.

Hasselmann, K., T. P. Barnett, E. Bouws, H. Carlson, D. E. Cartwright, K. Enke, J. A. Ewing, H. Gienapp, D. E. Hasselmann, P. Kruseman, A. Meerburg, P. Müller, D. J. Olbers, K. Richter, W. Sell and H. Walden, 1973: Measurements of wind-wave growth and swell decay during the Joint North Sea Wave Project (JONSWAP). *Dtsch. Hydrogr. Z., Ergänzungsheft Reihe A*, **12**, 95 pp.

——, D. B. Ross, P. Müller and W. Sell, 1976: A parametric wave prediction model. *J. Phys. Oceanogr.*, **6**, 200–228.

Kahma, K. K., 1979: On a two-peak structure in steady-state fetch-limited wave spectra. Phil. Lic. Study, Department of Geophysics, University of Helsinki, 77 pp.

——, 1981a: On the growth of wind waves in fetch-limited conditions. *Rep. Ser. Geophys.*, University of Helsinki, No. 15, 1–93.

——, 1981b: On prediction of the fetch-limited wave spectrum in a steady wind. *Finn. Mar. Res.*, **249** (in press).

——, and M. Leppäranta, 1981: On errors in wind speed observations on R/V *Aranda*. *Geophysica*, **17**, 155–165.

Kawai, S., K. Okada and Y. Toba, 1977: Support of the three-seconds power law and the $gu_*\sigma^{-4}$-spectral form for growing wind waves with field observational data. *J. Oceanogr. Soc. Japan*, **33**, 137–150.

Kitaigorodskii, S. A., 1962: Applications of the theory of similarity to the analysis of wind-generated wave motion as a stochastic process. *Izv. Akad. Nauk SSSR, Geophys. Ser.*, **1**, 105–117.

——, 1970: *The Physics of Air-Sea Interaction*. The English edition, 1973, A. Baruch, translator, P. Greenberg, Ed., Israel Program for Scientific Translations, 237 pp.

——, 1981: The statistical characteristics of wind-generated short gravity waves. The John Hopkins University, 9 pp.

——, and S. S. Strekalov, 1962: Contribution to an analysis of the spectra of wind-caused wave action. *Izv. Akad. Nauk SSSR Geophys.*, **9**, 1221–1228.

——, V. P. Krasitskii and M. M. Zaslavskii, 1975: On Phillips' theory of equilibrium range in the spectra of wind-generated gravity waves. *J. Phys. Oceanogr.*, **5**, 410–420.

Liu, P. C., and D. B. Ross, 1980: Airborne measurements of wave growth for stable and unstable atmospheres in Lake Michigan. *J. Phys. Oceanogr.*, **10**, 1842–1853.

Longuet-Higgins, M. S., 1969: On wave breaking and the equilibrium spectrum of wind-generated waves. *Proc. Roy. Soc. London*, **A310**, 151–159.

Mitsuyasu, H., 1969: On the growth of the spectrum of wind-generated waves (II). *Rep. Res. Inst. Appl. Mech. Kyushu Univ.*, **17**, 235–248.

——, 1977: Measurement of the high-frequency spectrum of ocean surface waves. *J. Phys. Oceanogr.*, **7**, 882–891.

——, and K. Rikiishi, 1978: The growth of duration-limited waves. *J. Fluid Mech.*, **85**, 705–730.

——, F. Tasai, T. Suhura, S. Mizuno, M. Ohkusu, T. Honda and K. Rikiishi, 1980: Observation of the power spectrum of ocean waves using a cloverleaf buoy. *J. Phys. Oceanogr.*, **10**, 286–296.

Moskowitz, L., 1964: Estimates of the power spectra for fully developed seas for wind speeds of 20 to 40 knots. *J. Geophys. Res.*, **69**, 5161–5179.

Pasquill, F., 1972: Some aspects of boundary layer description. *Quart. J. Roy. Meteor. Soc.*, **98**, 469–494.

Phillips, O. M., 1958: The equilibrium range in the spectrum of wind-generated waves. *J. Fluid Mech.*, **4**, 426–434.

——, 1977: *The Dynamics of the Upper Ocean*, 2nd ed. Cambridge University Press, 336 pp.

——, 1978: Strong interactions in wind-wave fields. *Turbulent Fluxes through the Sea Surface, Wave Dynamics, and Prediction*, A. Favre and K. Hasselmann, Eds., Plenum, 373–384, New York.

——, and M. L. Banner, 1974: Wave breaking in the presence of wind drift and swell. *J. Fluid Mech.*, **66**, 625–640.

Pierson, W. J., and R. A. Stacy, 1973: The elevation, slope and curvature spectra of a wind roughened sea surface. NASA Contractor Rep. CR2247, Langley Research Center, 128 pp.

Rao, K. S., J. C. Wyngaard and O. R. Coté, 1974: The structure of the two-dimensional internal boundary layer over a sudden change of surface roughness. *J. Atmos. Sci.*, **31**, 738–746.

Shemdin, O. H., 1972: Wind-generated current and phase speed of wind waves. *J. Phys. Oceanogr.*, **2**, 411–419.

Snyder, R. L., and C. S. Cox, 1966: A field study of the wind generation of ocean waves. *J. Mar. Res.*, **24**, 141–178.

Toba, Y., 1973: Local balance in the air-sea boundary process III. *J. Oceanogr. Soc. Japan*, **29**, 209–220.

——, 1978: Stochastic form of the growth of wind waves in a single-parameter representation with physical implications. *J. Phys. Oceanogr.*, **8**, 494–507.

Wilson, J. R., 1975: The recording and analysis system used in the Canadian wave climate study. *Waverider Discussion, Proceedings of the Conference held at the National Institute of Oceanography 31 Jan–1 Feb 1972*, L. Draper, Ed., Nat. Inst. Oceanogr., 74–77.

Wu, J., 1975: Wind-induced drift currents. *J. Fluid Mech.*, **68**, 49–70.